John von Neumann Institute for Computing

Exchange Frequencies in 2D Solids: Example of Helium 3 Adsorbed on Graphite and the Wigner Crystal

Bernard Bernu, Ladir Cândido, David M. Ceperley

published in

Quantum Simulations of Complex Many-Body Systems: From Theory to Algorithms, Lecture Notes,
J. Grotendorst, D. Marx, A. Muramatsu (Eds.),
John von Neumann Institute for Computing, Jülich,
NIC Series, Vol. **10**, ISBN 3-00-009057-6, pp. 63-74, 2002.

http://www.fz-juelich.de/nic-series/volume10

Exchange Frequencies in 2D Solids: Example of Helium 3 Adsorbed on Graphite and the Wigner Crystal

Bernard Bernu[1], **Ladir Cândido**[2], **and David M. Ceperley**[3]

[1] Laboratoire de Physique Théorique des Liquides
UMR 7600 of CNRS, Université Pierre et Marie Curie
boite 121, 4 Place Jussieu, 75252 Paris, France
E-mail: bernu@lptl.jussieu.fr

[2] Instituto de Física de São Carlos, Universidade de São Paulo
13560-970 São Carlos, SP, Brazil
E-mail: ladir@if.sc.usp.br

[3] Department of Physics and NCSA University of Illinois
Urbana-Champaign, Urbana, IL 61801, USA
E-mail: ceperley@ncsa.uiuc.edu

In 2d solids of fermion particles, such as helium 3 or electrons, the low temperature physics is governed by spin exchanges, according to the Thouless theory. We present Path Integral Monte Carlo (PIMC) calculation of ring exchange energies on "clean" 2d crystals of both helium 3 and electrons. We see a remarkable similarity of the results in these two "opposite" systems. They are both ferromagnetic in the semi-classical limit (strong coupling) antiferro magnetic near melting transition where the relative exchange energies become equivalent.

1 Introduction

In spin-less 2d solids, the low temperature physics is governed by the low excitations, the phonons. They provide a specific heat in $(T/\theta_D)^2$ in two dimensions, where the Debye temperature θ_D measures typical kinetic energy of a particle in its local potential. When $T/\theta_D \ll 1$, we can consider particles at zero temperature. Helium 3 atoms as well as electrons have a very large zero point motion. They eventually exchange their position resulting in a spin exchange that will modify the thermodynamics. Note here that helium 3 has a spin 1/2 nuclear spin whereas its two electrons are in a total spin 0 state. In the following we will consider helium 3 as atoms with a spin 1/2 interacting through a pair potential, say the Aziz potential. In the clean 2d Wigner crystal, electrons interact through the bare Coulomb potential.

The simplest effective model describing spin exchanges is the Heisenberg model:

$$H_{\rm spin} = \sum_{<i,j>} JP_{ij} = \sum_{<i,j>} (2J\mathbf{S}_i.\mathbf{S}_j - \frac{1}{2}). \qquad (1)$$

where J is the energy associated to the spin permutation P, and the last equality holds for spin 1/2. Assuming that $J \ll \theta_D$, we look at the leading contribution of $H_{\rm spin}$ to the specific heat at large temperature (meaning $J \ll T \ll \theta_D$) which behaves as $(J/T)^2$. The crossover between a $1/T^2$ and a T^2 law has been well established in specific heat measurements of helium 3 adsorbed on graphite[1](see Fig. 1). We see here a clear difference in

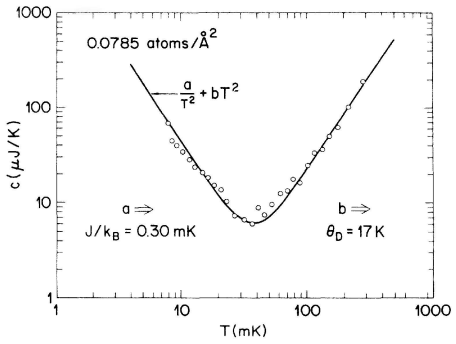

Figure 1. Specific heat measured by D. Greywall on 2d helium 3 adsorbed on graphite. One can see clearly the crossover between the spin contribution in $1/T^2$ and the phonon contribution in T^2.

energy scale between the degree of freedom associated to the spins and those associated to the spatial coordinates. In the intermediate regime $J \ll T \ll \theta_D$, particles can be considered both at zero temperature for their spatial degree of freedom, moving in their zero point motion, and without spin as they do not contribute anymore to the thermodynamics. In this intermediate regime we use Path Integral Monte Carlo on a spinless 2d solid system to evaluate ring exchange energies using a method first introduced by D. Ceperley for the three dimension solid of helium 3[2].

The full understanding of such a fermionic problem assume the Thouless theory can be applied[3]. In this approach, one consider the spin-less Hamiltonian in spatial coordinates. At low temperature, each particle oscillate with a zero point motion around a lattice position Z. If the particles are distinguishable, there are $N!$ possibilities of labeling the particles corresponding to $N!$ different points in the $2N$ dimensional phase space. If the barriers between those points would have been infinite the ground state would be $N!$ degenerate. Finite barriers allow tunneling effects between different points Z and PZ which differ in a permutation P of their coordinates (labeling). There is an energy J_P associated to such tunnel effect. The main point is that such an event is very rare ($J_P \ll \theta_D$) so that different permutations never occur simultaneously. Thus one can study each permutation separately. With PIMC, one evaluate the energy of the tunnel effect for various permutations. We find that usually not only the two body exchange is important but also the 3, 4, 5 and 6 exchanges have large contributions, specially near melting. In the semi-classical limit, WKB calculations provide useful informations[13,12], specially for the Wigner crystal[14].

The various ring exchange energies are accounted in the Multi spin Exchange (MSE) Heisenberg model:

$$H_{\mathrm{MSE}} = \sum_P J_P P. \tag{2}$$

This Hamiltonian lift the degeneracy of the spin-less Hamiltonian ground state. The eigen-

spectrum of this Hamiltonian has 2^N states that are the fermionic available states among the previous $N!$ states. The fermion problem is thus pushed at the level of the MSE model. Even if solving the MSE Hamiltonian is far from trivial, this is a simpler problem. Thus we solve this fermion problem in two steps. In the first one, PIMC is used on a spin-less solid to evaluate the exchange energies. Then those energies are introduced in the effective MSE Hamiltonian. Finally different techniques may be used to get informations on such Hamiltonian : exact diagonalizations[4], high temperature series expansion[5], spin wave or Schwinger bosons analysis[6], Quantum Monte Carlo[10], ...

The method to calculate exchange energy using PIMC has been already explained in details[8,9]. Results on 2d helium 3 on graphite are in Ref.[9]. The helium-graphite potential has a very deep well which leads to up to two solid layers. The helium-helium pair-potential interaction is short range and has a strong repulsive part and each layer solidifies on a triangular lattice. The density of each layer can be tuned by changing the total amount of helium in the system. Helium is the only liquid at very low temperature and the graphite can be made to have very flat surfaces of a few hundred angstrom wide. Therefore, this is a very "clean" system where comparisons between experiments and theories should agree. The semi-classical limit is at high density and the melting occur at density around $6\ nm^{-2}$. Results on the Wigner crystal can be found in Ref.[11]. The Coulomb interaction is smooth but long range. Therefore, the semi-classical limit (strong coupling) is at low density. The 2d solid is also a triangular lattice. Such system can be found at the surface of helium[15] or at the interface of semi-conductors[16]. Informations on the phase diagram of the resulting MSE model has been obtained from exact diagonalizations[4].

In the next section we recall the basic idea of how exchange energies can be calculated by PIMC. In the following section we introduce a reaction coordinate that map the problem on a one-dimensional system. In section 4, we study in more detail a double well problem.

2 PIMC Method

When the temperature is lowered, the crystal of electron attains its ground state and the low energy phonons are frozen. Each electron still has a zero point motion with a substantial kinetic energy. When one continues to decrease the temperature, electrons start to exchange their positions by tunneling, resulting in a spin exchange.

Because exchanges are very rare, each exchange can be studied independently. Suppose we label the particles. There are $N!$ such labeling. Starting with a given numbering, one chooses a given permutation P. In the phase space, we denote by Z the position of the original numbering and PZ the position of the permuted system. We are left here with a two well problem in a multi dimensional space. In this two well system the ground state ψ_0 of energy E_0 is symmetrical and the first excited state ψ_1 of energy E_1 is anti symmetrical. Other states have much higher energies. The diagonal density matrix element $< Z|\exp(-\beta H)|Z >$ and the off-diagonal density matrix element $< Z|\exp(-\beta H)|PZ >$ can be expanded as :

$$< Z|\exp(-\beta H)|Z > = \psi_0^2(Z)e^{-\beta E_0} + \psi_1^2(Z)e^{-\beta E_1} + \dots \quad (3)$$

$$< Z|\exp(-\beta H)|PZ > = \psi_0(Z)\psi_0(PZ)e^{-\beta E_0} + \psi_1(Z)\psi_1(PZ)e^{-\beta E_1} + \dots \quad (4)$$

$$= \psi_0^2(Z)e^{-\beta E_0} - \psi_1^2(Z)e^{-\beta E_1} + \dots \quad (5)$$

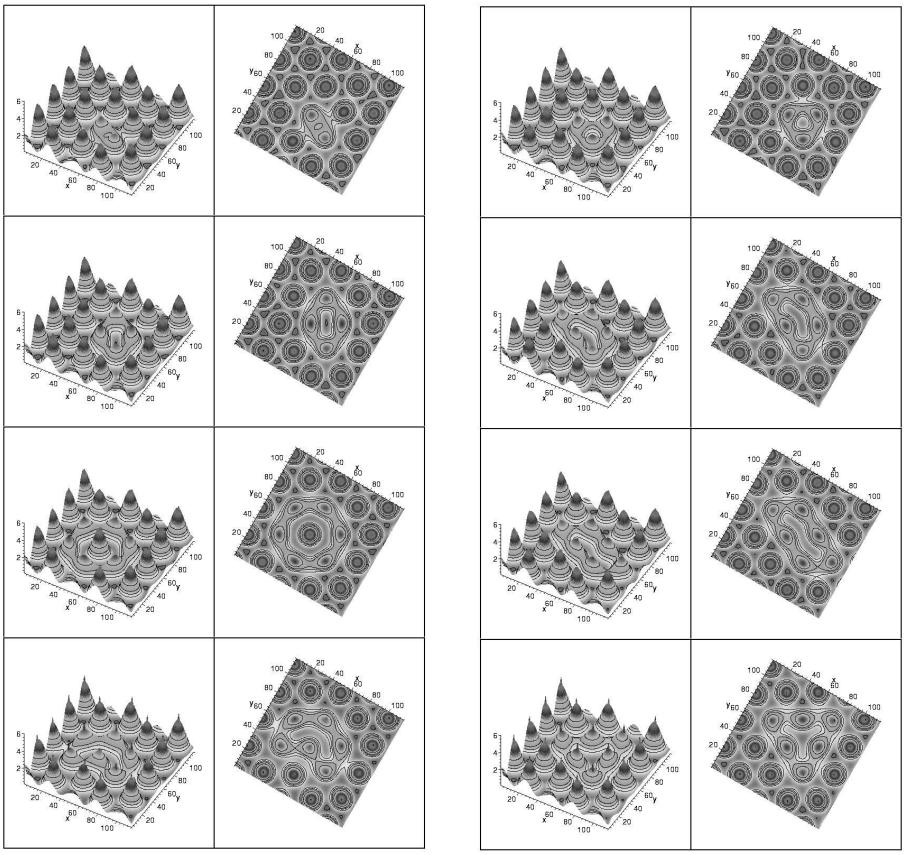

Figure 2. 3d plot of the one body density probability during exchanging paths for the Wigner crystal at $r_s = 40$, each data are represented from the side and from the top. The top 8 figures show 2, 3, 4 and 5 body exchanges, while the bottom 8 figures show the various 6 body exchanges. The "cones" represent the non exchanging particles. Notice that the center of mass of first neighbors of the exchanging particles are displaced from lattice position and their sizes are shrunken, especially in the 2 body exchange case. Note also the low probability density between electrons in the 6 body exchanges of the last row, indicating that those exchanges will be less probable.

where we have used the symmetry properties of the first two states. The ratio of these two density matrix elements is then:

$$F_P(\beta) = \frac{< Z|\exp(-\beta H)|PZ >}{< Z|\exp(-\beta H)|Z >} = \tanh(J_P(\beta - \beta_0)), \tag{6}$$

where J_P is the exchange frequency and $\beta_0 = \ln[\psi_1(Z)/\psi_0(Z)]$. Because $J_P\beta << 1$, one linearizes the previous equation and the slope of $F_P(\beta)$ gives the exchange energy. In terms of path integrals, one interprets $F_P(\beta)$ as the free energy necessary to make an exchange beginning with one arrangement of particles to lattice sites Z and ending on a permuted arrangement PZ. To evaluate $F_P(\beta)$, we use the method introduced by Bennett to calculate free energy differences of 2 chemical species A and B. The idea is to try to transform A in B and to calculate only the probability of success. Bennett[7] proposed an optimized scheme where one does 2 runs. The first one is an equilibrium run of A where the probability of finding B is calculated. The second run is the reverse. Here run A will be the non permuting system and run B will be the permuted one. In A, we evaluate the probability of successful exchanges P and in B the probability of successful identity. The energy of each type of permutation is evaluated in an independent run. (More clever scheme can be certainly tried. More details can be found in refs.[8,2,9,11], specially on the optimized Bennett's method in ref.[9].

Fig. 2 shows the probability of presence of particle in the xy plane during exchanging paths. The first neighbors of exchanging particles must move away in order to free space to exchange paths (in particular, see the 2 body exchange). In this pictures are represented the most important exchanges. Larger cycles as well as exchanges including second neighbor will have significantly smaller contributions.

3 Reaction Coordinate

As seen in Fig. 2, the exchanging particles are mostly localized around there lattice sites. During exchanges, only a small part of the path is involved while the main part of the path stays around Z or PZ. The part of the path that does the exchange uses a *"small"* amount of imaginary time β_0. Such process is called an instanton. The instanton occurs at any time between 0 and β. In the WKB calculations, where β goes to infinity, one has to remove first this degeneracy. In PIMC calculations, we must also find this degeneracy. We verify this property by calculating the exchange energy at the various imaginary time t. But, because the beads at times 0 and β are kept fixed in PIMC, there is some effect when the instanton touch the time 0 or β. For $\beta > \beta_0$, we find eventually a plateau. At large β, it can take a huge amount of CPU before obtaining a nice plateau. It is indeed hard to move the instanton at different imaginary times.

In order to get insight in this process, we define a reaction coordinate that help to map this multi dimensional problem onto a one dimensional one. A reaction coordinate allows to determine which part of the path is close to Z or PZ or exchanging :

$$z(t) = \frac{(R(t) - Z).(PZ - Z)}{|PZ - Z|^2} \tag{7}$$

For $z(t)$ close to 0 (resp. 1), the path is close to Z (resp. PZ). The figure 3-a shows $z(t)$ for the paths of run B. The exchanges take place at all time $0 < t < \beta$, but most of the time $z(t)$ is around 0 or 1. A crossing time t_c is defined by $z(t_c) = 1/2$. In figure 3-b are represented the same paths as functions of $t - t_c$. We see that the exchanges take roughly the same time. Because the exchange is localized in imaginary time, they are called instantons. Fitting these curves with $\tanh(2t/\beta_0)$, one defines the time β_0 needed for the path to go from Z to PZ.

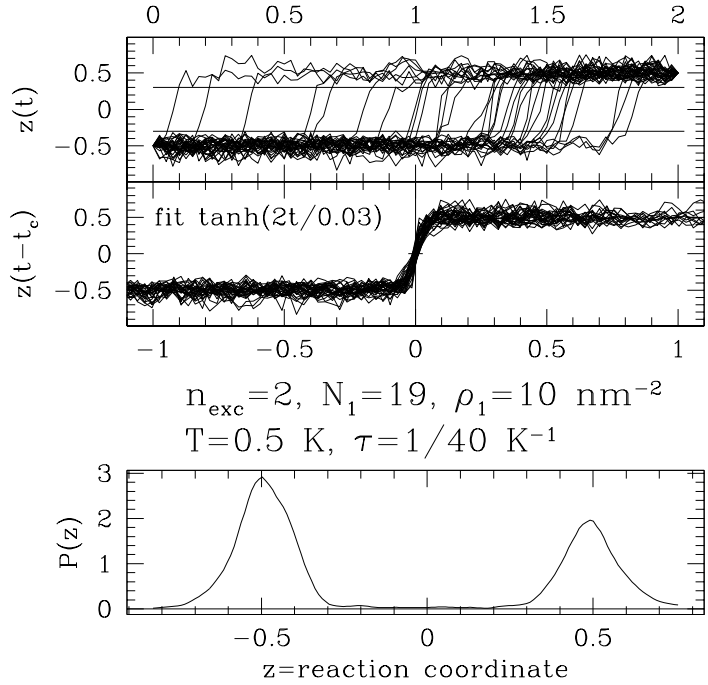

Figure 3. Reaction coordinate with respect to the time obtained in the B run. Only a few paths are used. top : row data where we see that exchange time arises at all possible time between 0 and β. middle : each path is now centered at the crossing time t_c. In bold solid line is the fit $\tanh(2t/\beta_0)$. bottom : probability of finding a value of z for these paths. The symmetry is due to the low number of paths used here.

The reaction coordinate can be used to map the $3N$ problem to a one dimensional one. First we build the probability distribution $P(z)$ from the value of $z(t)$, (see fig. 3-*c*). We define $\phi_0(z) = \sqrt{P(z)}$, where ϕ_0 is ground state of the Schrodinger equation $-\frac{1}{\phi_0}\frac{d^2\phi_0}{dz^2} = E_0 - U(z)$. The pseudo potential $U(z)$ is then fully determined assuming the ground state energy is $E_0 = 0$. The last step is to calculate the anti-symmetric states of this potential. The exchange energy (as well as the potential) is determined to a multiplicative constant λ which represent an effective mass associated with this reaction coordinate. The comparison of this mapping with the direct method fixes this mass λ.

4 A One Dimensional Toy Model: A Particle in a Symmetrical Double Well

As an example suppose, we have a single particle in a symmetrical double well potential. The Hamiltonian reads : $\mathcal{H} = -\lambda\nabla^2 + V$, where V is the potential shown in Fig. 4. The ground state ϕ_0 of energy E_0 is symmetric and the first excited state ϕ_1 of energy E_1 is anti-symmetric. A particle localized in the left well is described by $\phi_L = \frac{1}{\sqrt{(2)}}(\phi_0 + \phi_1)$ and in the right well by $\phi_R = \frac{1}{\sqrt{(2)}}(\phi_0 - \phi_1)$. Such a localized particle will oscillate between the left and right wells with a period $h/(E_1 - E_0)$. The time associated with the motion of the particle inside one of the wells is h/K where K is the kinetic energy of the

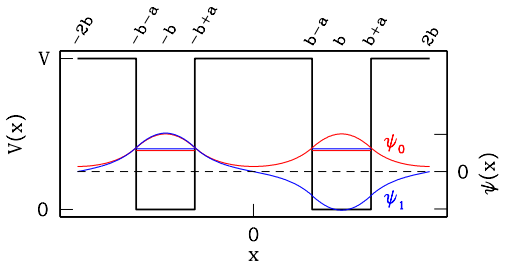

Figure 4. double well potential model. The ground state is a symmetrical function, whereas the first excited state, if it exists is antisymmetrical.

ground state. Let us suppose that $(E_1 - E_0) \ll K$. This means that the particle has a large number of zero-point vibrations in the left well before tunneling into the right well.

More generally, any permutation P may be view as a "particle" in two wells. The particle is the N-body system and the two wells represent the system around Z and PZ. The system of particles stay in the well around Z and eventually jump into the well PZ.

In order to understand how the exchange energies varies, we study the effects of the height V, the width $2a$ and separation $2b$ of the wells on the energy difference between the (symmetric) ground state and the first (anti-symmetric) excited state (see fig.4). For simplicity, we assume periodic boundary conditions.

Because of the periodic conditions and the symmetries of the wave functions, it is enough to study them in $[0, b]$ ($\psi(-x) = \pm\psi(x)$ and $\psi(b - x) = \psi(b + x)$). The ground state reads:

$$\psi_0(x) = A\cosh(x\sqrt{(V - E_0)/\lambda}) \qquad x \in [0, b - a] \tag{8}$$

$$\psi_0(x) = \ B\cos((x - b)\sqrt{E_0/\lambda}) \qquad x \in [b - a, b] \tag{9}$$

The coefficients A, B and E are determined by the continuity of the wave function and its derivative and the normalization condition. For $x = b - a$ we have:

$$A\cosh((b - a)\sqrt{(V - E_0)/\lambda}) = B\cos(a\sqrt{E_0/\lambda}) \tag{10}$$

$$A\sinh((b - a)\sqrt{(V - E_0)/\lambda})\sqrt{V - E_0} = B\sin(a\sqrt{E_0/\lambda})\sqrt{E_0} \tag{11}$$

The energy E_0 is the solution of the ratio of Eqs.10-11:

$$\tanh((b - a)\sqrt{(V - E_0)/\lambda})\sqrt{V - E_0} = \sqrt{E_0}\tan(a\sqrt{E_0/\lambda}) \tag{12}$$

Note that E_0 is also the ground state energy in a single periodic square well. The normalization condition reads:

$$A^2\left(\frac{\sinh(2(b - a)\sqrt{(V - E_0)/\lambda})}{\sqrt{(V - E_0)/\lambda}} + 2(b - a)\right) + B^2\left(\frac{\sin(2a\sqrt{E_0/\lambda})}{\sqrt{E_0/\lambda}} + 2a\right) = 1. \tag{13}$$

The ground state kinetic energy is given by:

$$K_0 = \frac{1}{2}\frac{\sqrt{(V-E_0)/\lambda}E_0\,(Va-(V-E_0)bX)}{(\sqrt{(V-E_0)/\lambda}a+\sqrt{(1-X)})V+X\sqrt{(V-E_0)/\lambda}(bE_0-aV)}, \qquad (14)$$

where $X = 1-\tanh^2((b-a)\sqrt{(V-E_0)/\lambda})$. For small X, one finds $K_0 = \frac{1}{2}E_0 a\sqrt{(V-E_0)/\lambda}/(a\sqrt{(V-E_0)/\lambda}+1)$.

Similarly, the first excited state is defined by :

$$\psi_1(x) = A\sinh(x\sqrt{(V-E_1)/\lambda}x) \qquad x\in[0,b-a] \qquad (15)$$

$$\psi_1(x) = \quad B\cos((x-b)\sqrt{E_1/\lambda}) \qquad x\in[b-a,b+a] \qquad (16)$$

E_1 is solution of :

$$\frac{\sqrt{V-E_1}}{\tanh((b-a)\sqrt{(V-E_1)/\lambda})} = \sqrt{E_1}\tan(a\sqrt{E_1/\lambda}) \qquad (17)$$

Let us define the splitting energy by $E_1 = E_0+\delta$. Inserting this definition in Eq. (17) and using Eq. (12), we get to the leading contribution in δ:

$$\delta = 8\frac{(V-E_0)E_0e^{-2(b-a)\sqrt{(V-E_m)/\lambda}}}{V(a\sqrt{(V-E_0)/\lambda}+1)}. \qquad (18)$$

The ratio δ/K_0 reads:

$$\frac{\delta}{K_0} = 16\frac{V-E_0e^{-2(b-a)\sqrt{(V-E_0)/\lambda}}}{Va\sqrt{(V-E_0)/\lambda}}. \qquad (19)$$

Fig. 5 shows the variations of these quantities with respect to the potential height V and the distance $2(b-a)$ between the wells (V is measured in units of λ/a^2.

When V increases to infinity, E_0 approaches $\lambda(\pi/2a)^2$, K_0 goes to $E_0/2$ and $\delta\sim 8E_0e^{-2(b-a)\sqrt{V/\lambda}-\ln(a\sqrt{V/\lambda})}$. The main dependence in $\log(\delta)$ is $-2(b-a)\sqrt{V/\lambda}$, where $2(b-a)$ represents the width of the barrier. The formula of Eq. (18) is accurate for $(b-a)V/\lambda > 1$. The exchange energy is thus exponentially small with the distance between the wells and with the square root of the potential height.

One can have a large potential barrier, when V is much larger then E_m. But one can also consider a large *kinetic* barrier when V/E_m is or order of unity but the width $b-a$ of the barrier is large.

5 Results and Magnetic Phase Diagram

At strong coupling (high density for helium and low density for electrons), semi-classical (WKB) calculations are accurate. For electrons, the exchange energies are given by[12,14]:

$$J_P = A_P b_P^{1/2} r_s^{-5/4} e^{-b_P r_s^{1/2}}. \qquad (20)$$

where $b_P r_s^{1/2}$ is the minimum value of the action integral along the exchanging path. This suggests to to plot J_p versus $r_s^{1/2}$ as it is shown in Fig. 6. At large r_s, the 3-body exchange is dominant leading to a ferro magnetic ground state.

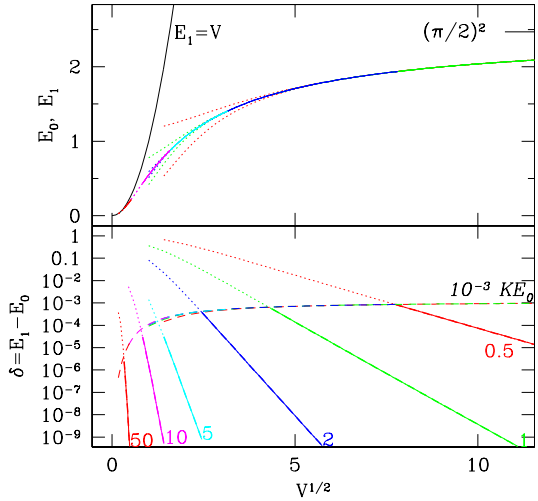

Figure 5. Top : Energies E_0 and E_1 versus V in units of λ/a^2 for $(b-a)/a = 1/2, 125$. Bottom : $\delta = (E_1 - E_0)$ and 10^{-3} times the kinetic energy.

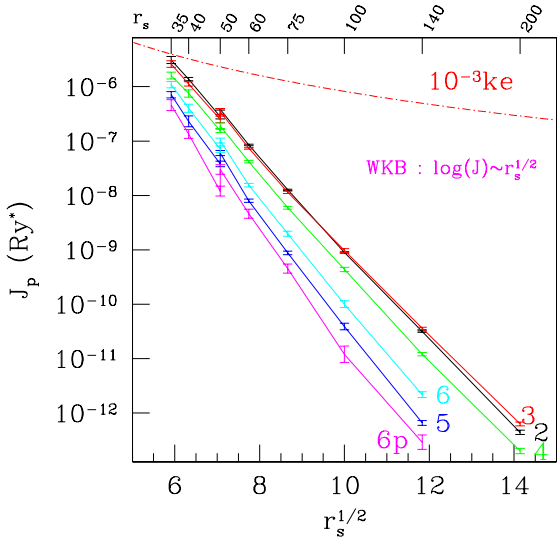

Figure 6. Exchange energies versus $r_s^{1/2}$. For $r_s \geq 50$ non exchanging electrons are distinguishable, and for $r_s \leq 50$, there are polarized (preliminary results). One can see that near melting, exchange energies become comparable with the kinetic energy.

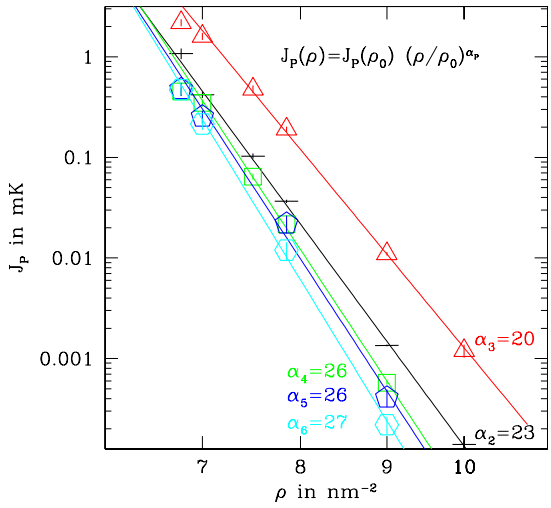

Figure 7. Helium 3 adsorbed on graphite: first layer exchange frequencies versus the density.

For helium 3 adsorbed on graphite, we find also strong variations with the density as shown in Fig. 7. The 3-body exchange is dominant for all densities and its exponent is also the smallest. This imply a ferromagnetic ground state at high density.

For both cases, at intermediate coupling the other 2, 4, 5 and 6 body exchanges are more and more important as the system approaches the melting transition. We put all these exchanges in the Hamiltonian defined in Eq. (2). The ferromagnetic 3 and 5 body exchanges are in competition with the antiferromagnetic 2, 4 and 6 ones. The nature of the ground state is sensitive to there relative values. The phase diagram of this Hamiltonian, obtained from exact diagonalization, is shown Fig. 8[4]. For spin 1/2, the 3 body permutations can be written in terms of pair permutations defining an effective pair permutation $J_2^{\rm eff} = J_2 - 2J_3$ which can be positive or negative. Thus we choose J_4 to scale energies and we are left with 3 parameters : $J_2^{\rm eff}/J_4$, J_5/J_4 and J_6/J_4. The straight lines in Fig. 8 separates the ferromagnetic (F) region from the antiferromagnetic (AF) one. The "trajectories" of the Wigner crystal and the second solid layer of helium 3 adsorbed on graphite crosses the F-AF transition line. In the AF region, no long range order has been found but on the contrary they are in a spin liquid state with a gap in all excitations[4,6].

A remarkable feature is the similarity of the relative exchanges (the trajectories are closed to each other), in particular when approaching the melting transition. Yet the interactions of these two systems are very different from a short range strongly repulsive potential for helium to a long range smooth potential for electrons. The search of an underlying universal mechanism is thus highly desirable (possibly virtual vacancy-interstitial (VI) mechanism[13]).

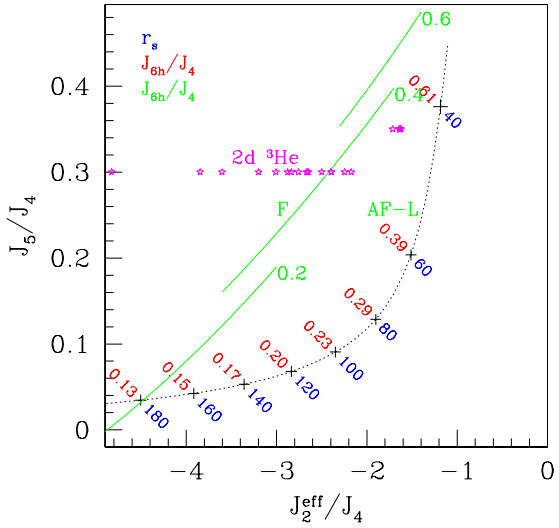

Figure 8. Zero temperature magnetic phase diagram of the MSE hamiltonian[4].

6 Conclusion

For fermionic solids, PIMC allows to evaluate exchange energies. These energies are then introduced in a MSE hamiltonian which in turn can be studied by different techniques. It is found that various two dimensional systems have a dominant 3 body exchange in the semi-classical limit (strong coupling) leading to a ferromagnetic ground state. As the quantum kinetic contributions increase, all exchanges become comparable with competitive ferro and antiferro interactions. Near melting it is found that the relative exchanges in the Wigner crystal are very similar with those obtained for a solid layer of helium 3 adsorbed on graphite, suggesting a possible universal behavior of the exchange mechanism near the melting transition.

References

1. D. S. Greywall and P. A. Busch, *Phys. Rev. Lett.* **65** 2788 (1990); D. S. Greywall *Phys. Rev. B* **41** 1842 (1990).
2. D. M. Ceperley and G. Jacucci, *Phys. Rev. Lett.* **58**, 1648 (1987).
3. D. J. Thouless, *Proc. Phys. London* **86**, 893 (1965).
4. G. Misguich, B. Bernu, C. Lhuillier and C. Waldtmann. *Phys. Rev. Lett.* **81** 1098 (1998); *Phys. Rev. B* **60** 1064 (1999).
5. M. Roger, C. Bauerle, Yu. M. Bunke, A.-S. Chen and H. Godfrin, *Phys. Rev. Lett.* **80**, 1308 (1998).

6. G. Misguich, B. Bernu and C. Lhuillier. *Journal of Low Temperature Physics* **110**, 327 (1998).
7. C. H. Bennett, *J. Comput. Phys.* **22** 245 (1976).
8. D. M. Ceperley, *Rev. Mod. Phys.* **67**, 279 (1995).
9. B. Bernu and D. Ceperley in *Quantum Monte Carlo Methods in Physics and Chemistry*, eds. M. P. Nightingale and C. J. Umrigar, Kluwer (1999).
10. S. Sorella, *Phys. Rev. B* **64** 024512 (2001), *Phys. Rev. B* **61** 2599 (2000).
11. B. Bernu, L. Candido, D. Ceperley *Phys. Rev. Lett.* **86** 870 (2001).
12. M. Roger, *Phys. Rev. B* **30** 6432 (1984).
13. M. Roger, J. H. Hetherington and J. M. Delrieu, *Rev. Mod. Phys.* **55** 1 (1983).
14. K. Voelker, S. Chakravarty, (cond-mat/0107151).
15. C. C. Grimes and G. Adams, *Phys. Rev. Lett.* **42**, 795 (1979).
16. J. Yoon *et al.*, *Phys. Rev. Letts.* **82**, 1744 (1999).